INTERNATIONAL JOURNAL OF ENERGY RESEARCH
Int. J. Energy Res. 2008; **32**:242–254
Published online 7 June 2007 in Wiley InterScience
(www.interscience.wiley.com) DOI: 10.1002/er.1344

Sensitivity of long-term performance simulations of solar energy systems to the degree of stratification in the thermal storage unit

Diego A. Arias, Andrew C. McMahan and Sanford A. Klein*,†

Solar Energy Laboratory, Department of Mechanical Engineering, The University of Wisconsin-Madison, 1500 Engineering Drive, Madison, WI 53706, U.S.A.

SUMMARY

This paper investigates the sensitivity of the long-term performance simulations of solar energy systems to the degree of stratification in both liquid and packed-bed storage units. The degree of stratification is controlled by the number of nodes used in a finite-difference approximation of the storage system temperature distribution. Short- and long-term simulations of typical water heating and solar thermal power plant systems are conducted. The results indicate that the long-term performance of these systems is far less sensitive to the number of nodes used to represent the degree of stratification than expected based on short-term simulations or experimental data. An explanation is offered for this non-intuitive result. Copyright © 2007 John Wiley & Sons, Ltd.

KEY WORDS: solar energy; thermal storage; stratification; long-term simulations

1. INTRODUCTION

Thermal energy storage is an important consideration in solar energy systems since solar energy availability and thermal energy demand are usually not coincident. Thermal energy can be stored as sensible energy in liquid storage tanks and in tanks that are filled with a porous media such as pebbles. In either case, the performance of the system is usually affected by the degree of thermal stratification that can be maintained in the storage unit. Mixing of stored energy at different temperatures has an adverse affect on system performance. Consequently, storage units are designed to maximize stratification. In a water storage tank, for example, stratification occurs naturally since warm fluid has a lower density than colder fluid. The system is usually designed so that hot fluid is provided at the top of the tank and cold fluid is provided at the bottom so as to enhance stratification. A similar situation occurs in packed beds although in this case, stratification does not directly depend on the density of the fluid but rather on the direction of flow of the fluid during the charging and discharging operations. Perfect stratification is not obtainable since mixing, axial

*Correspondence to: Sanford A. Klein, Solar Energy Laboratory, Department of Mechanical Engineering, The University of Wisconsin-Madison, 1500 Engineering Drive, Madison, WI 53706, U.S.A.
†E-mail: klein@engr.wisc.edu

Received 1 September 2006
Revised 1 December 2006
Accepted 21 January 2007

conduction and thermal losses always occur to some degree. However, with care, a high degree of stratification can be maintained in a storage unit by designing tanks with low inlet and outlet velocities as demonstrated by Gari and Loehrke [1] and Van Koppen *et al.* [2].

The performance of all solar energy systems is dependent upon the weather. The weather may be viewed as time-dependent boundary conditions that are neither completely random nor deterministic. The weather is best described as irregular functions of time on both short (e.g. seconds, minutes) and long (e.g. months and years) time scales. It is this irregular behaviour of the weather that complicates the analyses of solar energy systems. Since the weather cannot be controlled, repeatable experiments are difficult over long-term conditions. It is for this reason that simulations are most useful for the design of solar energy systems. However, simulations of solar energy systems can be computationally expensive because of the need for simulating the system performance at short intervals over long periods of time.

Models of both liquid and packed-bed storage units have been developed and validated with comparisons to experimental data. The governing equations for the storage units are partial differential equations that require numerical finite-difference solutions. The ability of these models to represent the stratification observed in experiments depends on the number of discrete sections or nodes used in the simulation model. Increasing the number of nodes provides greater stratification and better agreement with short-term experimental data, such as that provided by Zurigat *et al.* [3] Mavros *et al.* [4] Drück *et al.* [5] and others. Hundreds of nodes are usually needed to closely represent the stratification that is observed in experimental data. However, the computation expense of a storage model used for long-term performance studies increases with the number of nodes employed.

This paper investigates the sensitivity of the long-term performance simulations of solar energy systems to the number of nodes used in both liquid and packed-bed storage units. Short- and long-term simulations of typical water heating and solar thermal power plant systems are conducted. The results indicate that the long-term performance of these systems is far less sensitive to the number of nodes used to represent the degree of stratification than expected based on short-term simulations and experimental data. An explanation is offered for this non-intuitive result.

2. WATER STORAGE SYSTEMS

The hot water storage tank is one of the key elements of a solar heating system. The tank has to fulfil several tasks, such as delivering sufficient energy to the load in the form of mass flow rate and temperature, decoupling the heat source and load mass flow rates, providing energy to or from unsteady heat sources during times when there is either too little or excess resource available, and allowing a reduction in the required heating capacity of auxiliary heating devices [6]. This section presents a one-dimensional model of liquid storage tanks, which is used in a simulation of a complete solar domestic water heating system. The sensitivity of the integrated results over a long period of time is determined with respect to the number of nodes in the tank and the length of the simulation.

2.1. Water storage tank model

The thermal performance of a liquid storage tank subject to thermal stratification can be modelled by assuming that the tank consists of N fully mixed volume elements as described by Kleinback *et al.* [7] and Duffie and Beckman [8]. Figure 1 shows the internal flows associated with node i. This model assumes that $\dot{m}_1$ is added to $\dot{m}_4$ in an adiabatic mixing operation resulting in a net flow up or down. Similarly, $\dot{m}_2$ is added to $\dot{m}_3$. An energy balance written on the ith tank node is given by

$$\begin{aligned} M_i C_f \frac{dT_i}{dt} = {} & \alpha_i \dot{m}_{heat} C_f (T_{heat} - T_i) \\ & + \beta_i \dot{m}_{load} C_f (T_{mains} - T_i) \\ & + \delta_i \gamma_i C_f (T_{i-1} - T_i) \\ & + (1 - \delta_i) \gamma_i C_f (T_i - T_{i+1}) + \epsilon \dot{Q}_{aux,i} \\ & - UA_i (T_i - T_{env}) \end{aligned} \quad (1)$$

DOI: 10.1002/er

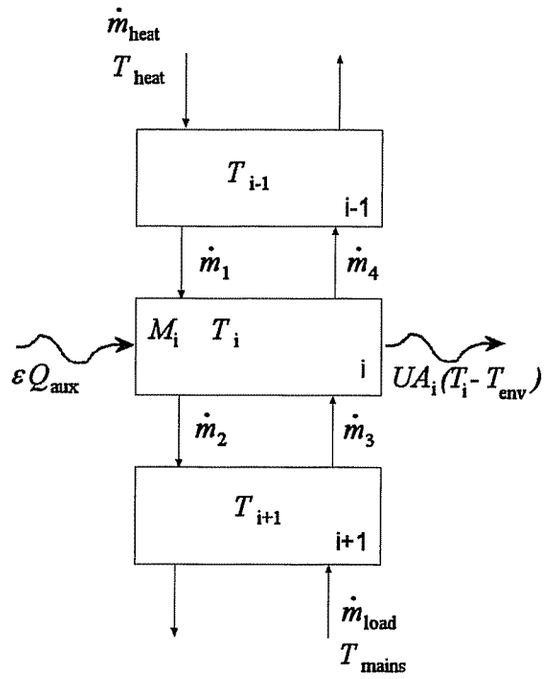

Figure 1. Internal flows into node i. Adapted from Kleinback *et al.* [7].

where T_i is the temperature of the node, T_{heat} is the temperature of the fluid from the heat source, T_{mains} is the mains water temperature, T_{env} is the temperature of the environment, M_i is the mass of fluid in the node, C_f is the heat capacity of the fluid, $\dot{m}_{heat}$ and $\dot{m}_{load}$ are the fluid flow rates from the heat source and to the load, respectively, $\dot{Q}_{aux,i}$ is the rate of auxiliary energy input into node i, UA_i is the heat loss coefficient of the tank corresponding to node i, $\alpha_i = 1$, if fluid from heat source enters node i, 0 otherwise, $\beta_i = 1$, if fluid returning from load enters node i, 0 otherwise,

$$\gamma_i = \dot{m}_{heat} \sum_{j=1}^{i-1} \alpha_j - \dot{m}_{load} \sum_{j=i+1}^{N} \beta_j$$

$$\delta_i = \begin{cases} 1 & \text{if } \gamma_i > 0 \\ 0 & \text{if } \gamma_i \leqslant 0 \end{cases}$$

and $\epsilon = 1$, if auxiliary heater is on, 0 otherwise.

Several studies have found the need for a large number of nodes in order to fully capture the effect of stratification in the tank (e.g. Mavros *et al.* [4], Obendorfer *et al.* [9]). For example, using experimental data provided by Drück at University of Stuttgart, Obendorfer *et al.* found that 100 or more nodes are required to reproduce the degree of stratification observed during short-term experiments. However, fewer nodes may be sufficient to capture the long-term performance of the system. The following sections present the results of long-term simulations, in which several parameters are changed in order to compare the performance of the system predicted with a tank model with 1, 2, 6, 15 and 50 nodes.

2.2. *Validation of the storage tank model*

Newton [10] compared the results of the one-dimensional model with the experimental results obtained by Zurigat *et al.* [3]. The experimental set-up of Zurigat *et al.* consisted of an insulated steel test tank (2.5 mm thick wall with 7.62 cm of fibreglass insulation) in which hot water at a constant temperature of 89°C entered at the top of the tank at a flow rate of $0.1251\,s^{-1}$ (1.98 gpm). The tank was initially at a constant temperature of 19°C. The test was a single charge cycle in which water was drawn into the tank until the entire tank reached a constant temperature. Figure 2(a) shows the dimensions of the tank and the location of the thermocouples for comparison with the computer model. Figure 2(b) compares the experimental temperature profiles with the results of the one-dimensional model at the different thermocouple heights. The one-dimensional model was solved with different number of nodes, and it was found that 100 or more nodes were required in order to closely represent the observed stratification in the tank, consistent with the results of Obendorfer *et al.* [9]. In order to ensure the stability of the solution, a time step equal to 6 min was used to simulate the tank with 100 nodes. The solution of the model with fewer nodes resulted in a skewed temperature profile showing reduced stratification when compared with the experiments. A logical conclusion of this study is that many (100 or more)

DOI: 10.1002/er

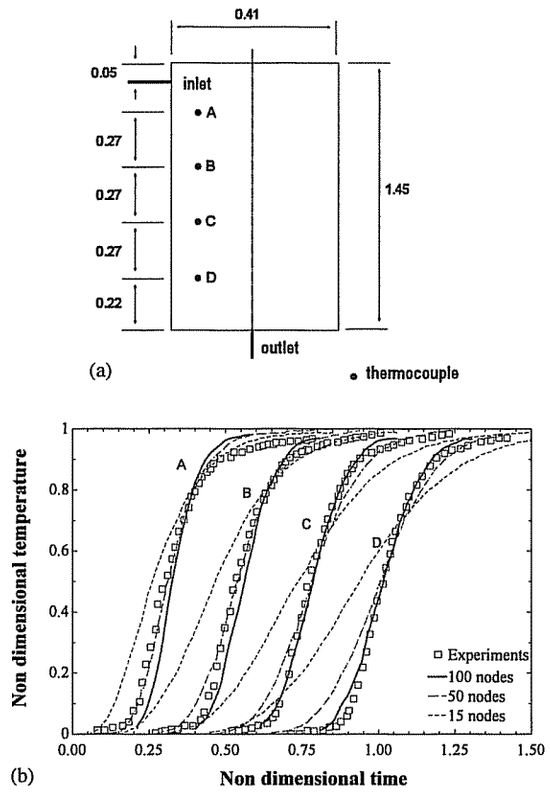

Figure 2. Experimental validation of one-dimensional tank model: (a) dimensions of water tank (in meters) and (b) non-dimensional temperature distribution inside tank with different number or nodes and experimental results. Adapted from Newton [10].

nodes are needed to accurately represent the stratification in a water storage tank.

2.3. *Long-term simulation results for water storage systems*

In order to study the effect of the number of nodes in the one-dimensional tank model, a solar domestic water heating system as shown in Figure 3(a) was simulated in TRNSYS [11]. The main energy source was a single-cover solar collector having an area of $4\,m^2$, and efficiency curve characterized by an intercept of 0.8 and slope of $3.61\,Wm^{-2}\,K^{-1}$. Water was pumped through the collector loop at a flow rate of $2001\,h^{-1}$ when the

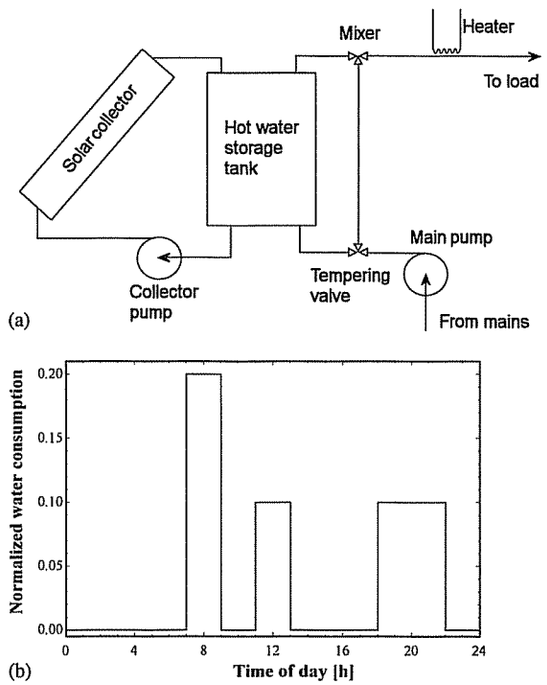

Figure 3. (a) Solar domestic water heating system simulated in TRNSYS and (b) normalized water consumption schedule.

solar radiation was high enough to increase the water temperature in the tank. The hot water storage tank had a volume of $0.3\,m^3$, which corresponds to a standard storage capacity of 751 of stored water per square meter of collector area [8]. Water was drawn from the water mains at 15°C. The average daily water consumption was $3001\,day^{-1}$, simulated with the normalized schedule shown in Figure 3(b). If the solar resource was not sufficient to heat the water to the set point of 45°C, an instantaneous heater placed after the mixer was activated as needed to meet the load. A tempering valve controlled the water temperature to the load to ensure that is was not above the set temperature.

The performance of the system is described in terms of the solar fraction F, defined by

$$F = 1 - \frac{\int_{t_0}^{t} Q_{\text{aux}}\,\mathrm{d}t}{\int_{t_0}^{t} \dot{m}_{\text{load}} C_{\text{f}} (T_{\text{set}} - T_{\text{mains}})\,\mathrm{d}t} \qquad (2)$$

DOI: 10.1002/er

where T_{set} is the hot water set temperature which was fixed at 45°C. A solar fraction equal to one indicates that all the energy required by the load is provided with the solar collector. On the other extreme, it is possible to have the auxiliary heater provide more energy than needed to meet the load in order to make up for the environmental losses; in this case, Equation (2) may yield a negative number for F.

Two sets of simulations were performed: first, hourly weather data corresponding to a typical meteorological year were used to simulate the effect of the variability of the environmental conditions during a year-long simulation. Second, several system parameters (such as collector size, tank size, daily water consumption and collector flow rate) were modified in order to verify that the sensitivity of the results to the number of nodes was consistent over a wide range of values. The system was simulated with a storage tank with different number of nodes, from 1 to 50. In order to ensure that the node size produced a stable solution, a time step of 15 min was used, which in all cases resulted in a Courant number below the critical value of 1 [12]. The results obtained with this time step were less sensitive to the use of smaller time steps than with respect to the number of nodes and other variables. Additional information relating to the time step and the Courant number is provided in Section 2.6.

2.3.1. Typical meteorological year simulations. Simulations were conducted using the weather conditions corresponding to a typical meteorological year for the city of Zurich (Switzerland). The use of actual weather data takes into account the variability of the boundary conditions, which prevents the system from reaching a dynamic steady state. Figure 4 shows the solar fraction as a function of time and number of nodes used to represent the tank. The storage tank was assumed to be at a uniform temperature at the start of the simulations. Initial tank temperatures of 20 and 50°C were assumed. However, the effect of the initial conditions becomes insignificant after ≈ 60 days. The difference in solar fraction between the 50-node and the 1-node tank is less than 0.07 after 60 days of simulation, while the difference in solar

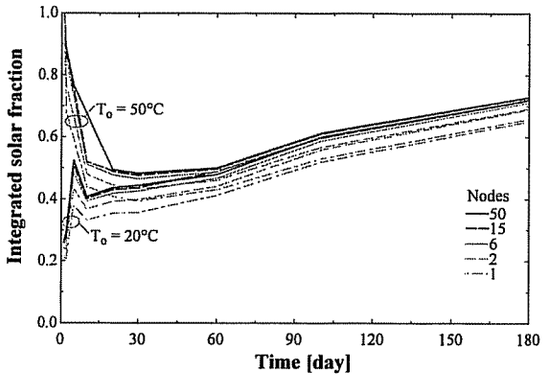

Figure 4. Effect of number of nodes on integrated solar fraction with initial uniform temperatures of 20 and 50°C.

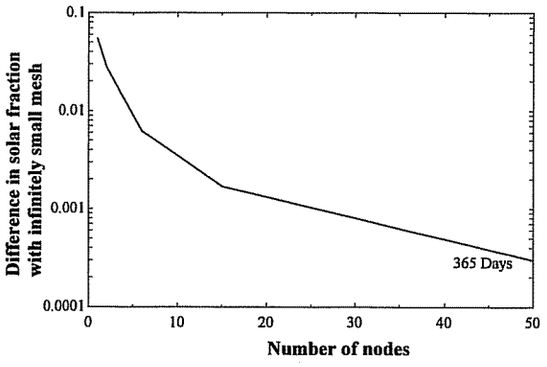

Figure 5. Difference in integrated annual solar fraction between a system with a finite node size and the extrapolated results with an infinitesimally small node size. The extrapolated results were calculated with Richardson extrapolation.

fraction between the 50-node and the 6-node tank is about 0.01.

Richardson extrapolation was used to calculate the annual solar fraction that would be obtained with an infinitesimally small node size [13]. This extrapolated value was used to determine the difference in annual solar fraction between the extrapolated value and that determined with a finite node size as shown in Figure 5. It was found that only a few nodes were required to reduce the calculated error in annual solar fraction to less than 0.05: these results are non-intuitive given that the single-day simulation results indicated that as

DOI: 10.1002/er

many as 100 nodes were needed to replicate the experimentally observed stratification.

2.4. *Effect of system parameters*

Several system parameters were varied in the simulation in order to investigate the sensitivity of the annual system performance to the number of nodes. The annual solar fraction was calculated with the weather data for the city of Zurich for different values of collector area, tank volume, daily water consumption and collector flow rate (see Figures 6 and 7). In all of the cases it was found that the differences between the results for the 1-node and the 50-node tank were less than 0.08. Furthermore, the results of solar fraction with a 6-node tank were within 0.01 of the results with a 50-node tank. In all the cases, these differences were almost constant, demonstrating that simulations conducted with storage represented with a few nodes yield a similar annual estimates to those obtained with a tank model that uses many nodes.

2.5. *Effect of time step*

The effect of time step was assessed by calculating the annual solar fraction with weather data for the city of Zurich for tanks with different number of nodes and time steps, as shown in Figure 8. The Courant number for the tank was below 1 in all cases (see Section 2.6). Richardson extrapolation

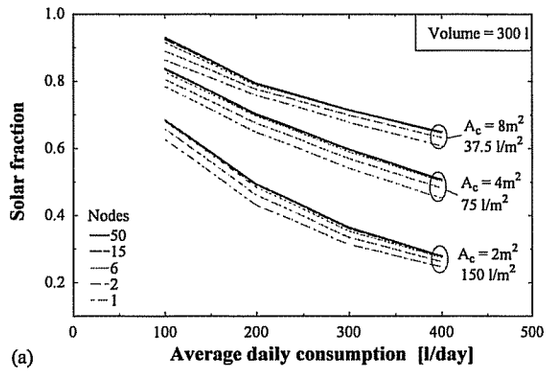

Figure 6. Effect of daily average water consumption, collector area and tank volume on annual solar fraction. Simulations performed with typical meteorological year for Zurich (Switzerland): (a) 300 l tank and (b) 400 l tank.

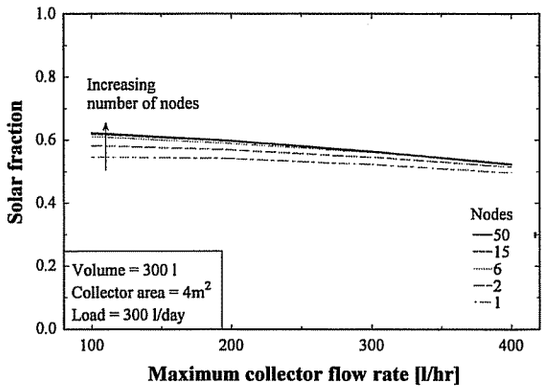

Figure 7. Effect of collector loop flow rate on annual solar fraction. Simulations performed with typical meteorological year for Zurich (Switzerland).

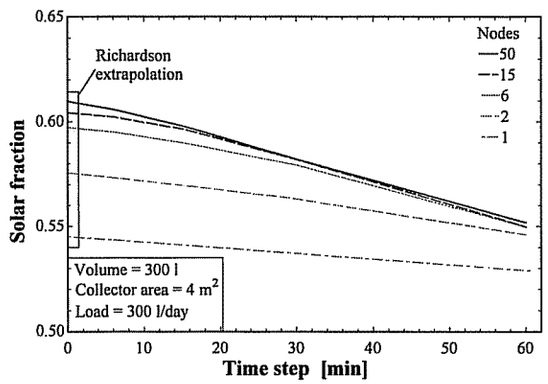

Figure 8. Effect of time step on annual solar fraction.

DOI: 10.1002/er

was used to calculate the annual solar fraction for an infinitesimally small time step. The annual solar fraction was found to be more sensitive to number of nodes than to the time step for these simulations, e.g. the 50-node tank exhibited a difference in solar fraction of 0.01 between the 15-min time step and the extrapolated value for an infinitesimally small time step, while the difference between the annual solar fraction (for an infinitesimally small time step) between a 50-node and a 1-node tank was about 0.05.

2.6. *Effect of number of nodes and time step on the total simulation time*

The total simulation time is affected by the number of nodes in the tank in two ways: first, a greater number of nodes in the tank require the solution of a greater number of equations. Second, an increased number of nodes may require a shorter time step in order to ensure the stability and convergence of the solution. This condition is met if the Courant number is less than one. The Courant number is defined by

$$\mathrm{Co} = \frac{v\,\Delta t}{\Delta x} \tag{3}$$

where Δt is the time step, Δx is the distance between nodes and v is the mean velocity inside the tank. This expression can be rewritten in terms of the maximum mass flow rate into the tank, $\dot{m}$, the fluid density, ρ, and the cross-sectional area of the tank A_c:

$$\mathrm{Co} = \frac{\dot{m}}{\rho A_c}\frac{\Delta t}{\Delta x} \tag{4}$$

This expression, based on the maximum mass flow rate into the tank, sets the most extreme condition for the Courant number. Any other combination of mass flow rates into and out of the tank will result in a smaller Courant number.

Simulations were performed with a constant time step of 0.25 h, which ensured that the Courant number was below 1. Figure 9 shows the total simulation time, normalized by the total simulation time of the solar system with a 1-node tank. When the simulations were performed with a constant time step of 0.25 h, the simulation time required by the 50-node tank was 2.3 times the simulation time of a 1-node tank. However, when the simulations were run with the time step required to maintain the same Courant number, the time required by the 50-node tank was 34 times the simulation time of a 1-node tank.

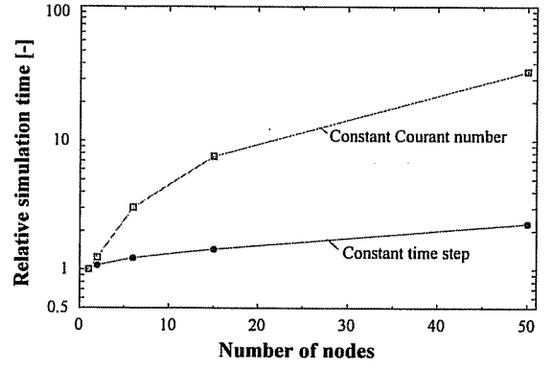

Figure 9. Effect of number of nodes and time step on the total simulation time. The total simulation time is normalized by the total simulation time of a system with a 1-node tank.

2.7. *Discussion of the solar water heating system results*

The results indicate that the solar fraction becomes less sensitive to the number of nodes used to represent the stratification in the storage tanks as the length of time of the simulation increases. The performance calculated with six nodes is very close to that found for 50 nodes for a one-year simulation, yielding a difference in solar fraction of about 0.01. The results of this study show that, although many nodes may be needed to duplicate the behaviour observed in a short-term experiment, a model with many fewer nodes (and thus less computational expense) is sufficient for determining long-term system performance. This finding indicates that in long-term simulations, the level of detail in which the temperature inside the tank is represented is less important than the overall energy balance on the system.

3. THERMAL POWER PLANT SYSTEMS

Solar thermal power plants, like domestic hot-water systems, are typically simulated over long

DOI: 10.1002/er

periods of time using models calibrated against short-term data. In this section a model is presented for the simulation of high-temperature packed-bed thermal storage tanks. The sensitivity of relevant simulation results to numerical precision is considered over varying time scales to investigate the connection between model calibration based on short-term data and long-term simulation results.

3.1. *Packed-bed thermal storage model*

The Schumann [14] model is a one-dimensional heat transfer model of fluid flow through a packed bed. It neglects axial conduction, viscous dissipation, temperature gradients within the solid particles and convective shell losses. These simplifications are appropriate for well-designed thermocline storage systems [15, 16]. The Schumann model takes the form of two coupled governing differential equations:

$$\dot{m}_f C_f \frac{dT_f}{dx} + \rho_f \epsilon A_c C_f \frac{dT_f}{dt} = -h_v A_c (T_f - T_s) \quad (5)$$

$$\rho_s (1-\epsilon) C_s \frac{dT_s}{dt} = h_v (T_f - T_s) \quad (6)$$

where $\dot{m}_f$ is the fluid flow rate, C_f is the specific heat capacity of the fluid, ρ_f and ρ_s are the densities of the fluid and solid material, respectively, ϵ is the void fraction, h_v is the volumetric fluid–solid heat transfer coefficient, A_c is the cross-sectional of the storage system, T_f and T_s are the temperatures of the fluid and solid, respectively, x is the spatial coordinate in the flow direction and t is time.

Storage systems intended for use in power plants use high-temperature oils or molten salts as the fluid storage medium along with rocks and sand as the solid material. Such a configuration results in substantial fluid–solid heat transfer surface area as well as much higher fluid–solid heat transfer coefficients than those observed in the more commonly modelled gas–solid systems. McMahan [15] showed that, based on this observation, it is appropriate to assume an infinite fluid–solid volumetric heat transfer coefficient in these systems. With this assumption, the fluid and solid are in thermal equilibrium ($T_f(x,t) = T_s(x,t)$) at all positions at any time. Applying the infinite heat transfer assumption to the Schumann model simplifies Equations (5) and (6) to a single homogeneous governing equation:

$$\dot{m}_f C_f \frac{\partial T}{\partial x} + (\rho_f \epsilon C_f + \rho_s (1-\epsilon) C_s) A_c \frac{\partial T}{\partial t} = 0 \quad (7)$$

Note that both the fluid and solid thermal capacitances are included in the time-derivative term. Fluid capacitance is often neglected when modelling gas–solid systems where the fluid thermal capacitance is small. However, the thermal capacitance of the liquid is significant relative to that for the solid in the liquid–solid systems used for power plant storage [15, 17]. Combining the two capacitance terms, as in Equation (7), accounts for the thermal capacitance effects in the fluid assuming thermal equilibrium between the solid and the fluid.

Equation (7) was solved using a single-step explicit numerical technique wherein the equation for each node during each time step is

$$\frac{\dot{m}_f C_f}{\Delta x}\left(\left(\frac{T_{(i-1,t)} + T_{(i,t)}}{2}\right) - \left(\frac{T_{(i,t)} + T_{(i+1,t)}}{2}\right)\right) = \frac{(\rho_f \epsilon C_f + \rho_s (1-\epsilon) C_s) A_c}{\Delta t} (T_{(i,t+1)} - T_{(i,t)}) \quad (8)$$

where

$$\Delta x = \frac{H}{N}, \quad \Delta t = \frac{\rho_f A_c \Delta x (1-\epsilon)}{\dot{m}_f} \quad (9)$$

In Equation (8), H is the height of the storage unit and N is the number of discretized sections used in the finite-difference approximation. Δt is defined such that the amount of fluid passing through a node in one time step is equal to the fluid capacity of a single node. Tying the time step to the node size allows overall numerical precision to scale in a uniform manner as the node size is varied.

Figure 10 shows the solution of Equations (8) and (9) for a case in which an initially isothermal storage tank is charged with a constant temperature flow for a fixed period of time. The system parameters are chosen to be representative of a power plant storage system. The fluid capacitance rate is $1.7\,\mathrm{MW\,K^{-1}}$ and the combined fluid–solid capacitance is $560\,\mathrm{MJ\,m^{-1}\,K^{-1}}$. The numerical solution clearly converges as the number of nodes

DOI: 10.1002/er

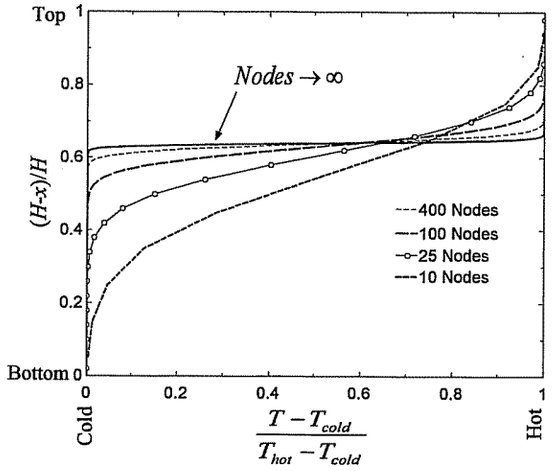

Figure 10. The numerical solution to Equation (7) converging on its analytical solution as the number of computational nodes increases.

increases. It appears from Figure 10 that at least 100 nodes are required to obtain a reasonable approximation of the converged temperature profile, and substantially more nodes are required to match it precisely.

3.2. Simulation results for thermal power systems

The model developed in the previous section was used to run a series of simulations. The objective of these numerical experiments is to determine whether the conclusions regarding the number of nodes needed for accurate results obtained for a single charge–discharge cycle apply to long-term performance calculations.

To describe the performance of the model over varying time scales it is necessary to define a metric that is relevant to the balance-of-system operation and applicable over short and long simulation periods. The model developed here is specific to storage systems designed for power generation. In power generation applications a convenient and appropriate measure of storage system performance is the second-law efficiency of the storage unit defined in the following manner:

$$\eta_{\text{2nd law}} = \frac{\int_{t_0}^{t} (\dot{\psi}_{\text{out,discharge}} - \dot{\psi}_{\text{in,discharge}})\,\mathrm{d}t}{\int_{t_0}^{t} (\dot{\psi}_{\text{in,charge}} - \dot{\psi}_{\text{out,charge}})\,\mathrm{d}t} \quad (10)$$

where $\dot{\psi}$ is the availability (exergy) rate of an incompressible fluid defined as:

$$\dot{\psi} = \dot{m}_{\text{f}}\left[C_{\text{f}}(T_{\text{f}} - T_0) - T_0 C_{\text{f}} \ln\left(\frac{T_{\text{f}}}{T_0}\right)\right] \quad (11)$$

Availability is the theoretical upper limit on the amount of work that can be extracted from a thermal resource. The second-law efficiency of the storage unit represents the percentage of potential work, delivered to the storage system during charging, that is recovered during discharging. Availability is destroyed when fluids of different temperatures are mixed. This mixing causes the temperature of the fluid discharged from the storage system to be lower than it was during charging.

As seen in Figure 10, the infinite heat transfer model converges to a perfectly stratified storage system since internal mixing and axial conduction effects are assumed to not occur. A perfectly stratified storage system would attain a 100% second-law efficiency, since the absence of mixing and conduction effects results in no availability being destroyed.

3.3. Discussion of the thermal power system simulation results

Figure 11 shows the results of three sets of simulations for which the error in the predicted second-law efficiency is calculated as a function of the number of computational nodes. The error is defined as:

$$\text{error} = \frac{|\eta_{\text{ref}} - \eta|}{\eta_{\text{ref}}} \quad (12)$$

where η is the second-law efficiency for a system with finite number of nodes, and η_{ref} is the second-law efficiency of a system with infinite number of nodes.

The first set of simulations (solid circles) is a single charge–discharge cycle, where an isothermal storage tank is charged at constant flow rate and temperature long enough to replace ~ 75% of the initial fluid capacity. The tank is then discharged for an equal period of time at the same flow rate. The second set of simulations (open circles) uses the same charge–discharge cycle, but instead reports the second-law efficiency integrated over

DOI: 10.1002/er

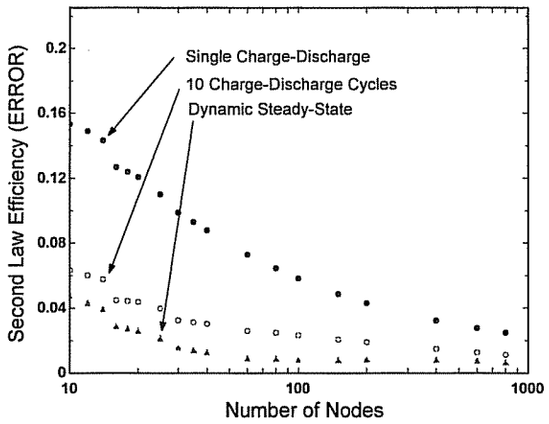

Figure 11. Error in the computation of second-law efficiency as a function of the number of numerical nodes for three cases: a single charge–discharge cycle; 10 identical charge–discharge cycles; and the calculation of dynamic steady-state storage system efficiency.

10 cycles. The final set of simulations (triangles) shows the error in calculating the dynamic steady-state efficiency of the storage system. The dynamic steady state can be viewed as the result of an infinite number of charge–discharge cycles, since the system performance eventually arrives at a dynamic equilibrium condition where predicted storage system efficiency does not change from one cycle to the next.

The single-cycle second-law efficiency shows an error of about 15% in Figure 11 for the 10-node simulation and a single charge–discharge cycle. The 15% error in second-law efficiency seems extremely modest considering how poorly the 10-node temperature profile compares to the converged solution in Figure 10. Tank temperature profiles are a convenient way to match models with experimental data or analytical solutions, but the error in these profiles may not be indicative of the error in the calculated long-term performance.

In Figure 11, the single-cycle case shows substantially more error than either the 10-cycle or the dynamic steady-state simulations. This observation demonstrates that, although a numerical solution with a given number of nodes may do a poor job of predicting the single-cycle performance of the storage system, over time the error associated with this initial prediction is mitigated. It is apparent, then, that the number of nodes required to achieve a desired degree of accuracy over longer simulation periods is smaller than would be expected based on the temperature profile or single-cycle results. For example, if 4% second-law efficiency error were the accuracy target, more than 400 nodes would be required for a single-cycle simulation. However, only 50 nodes would be needed for 10 cycles and 20 for dynamic steady-state operation.

In order to understand why the error is reduced over time, the temperature profiles for two simulations are considered: one with 600 nodes and one with 20 nodes. Figure 12(a) shows the results for the 600-node simulation. After the initial charge (from isothermal conditions) there is nearly perfect stratification since the large number of nodes provides a close approximation of the analytical solution. As a result, the 600-node simulation generates little error over both a single cycle and the long term. Note that the temperature profiles change very slightly from cycle to cycle, rapidly converging on the dynamic steady-state solution. Note also that the minimum discharge temperature (the temperature at which the discharged temperature profile intersects with the top of the tank) increases as the number of cycles increases. This increase in minimum discharge temperature results in an increase in second-law efficiency, and a better approximation of the analytical solution (100%).

Figure 12(b) shows similar results for the 20-node simulation. The 20-node simulation also approaches steady-state temperature profiles, but it does so through much larger variation in the first several cycles. The large variation in temperature profiles results in a larger increase in the minimum discharge temperature, and a subsequently larger change in long-term error observed in Figure 11.

The large variation in minimum exit temperature in the 20-node model is a result of the energy that is 'stranded' at the top of the tank during the first discharge cycle. This energy would have been discharged in the converged model. The 'stranded' energy serves as the initial condition for the following cycles which triggers the increase in minimum outlet temperature, and the subsequent decrease in second-law efficiency error.

DOI: 10.1002/er

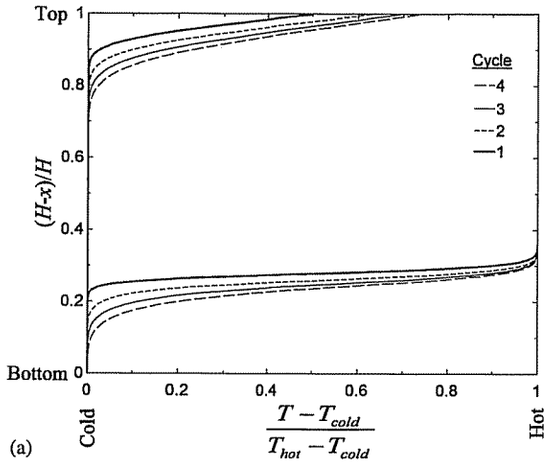

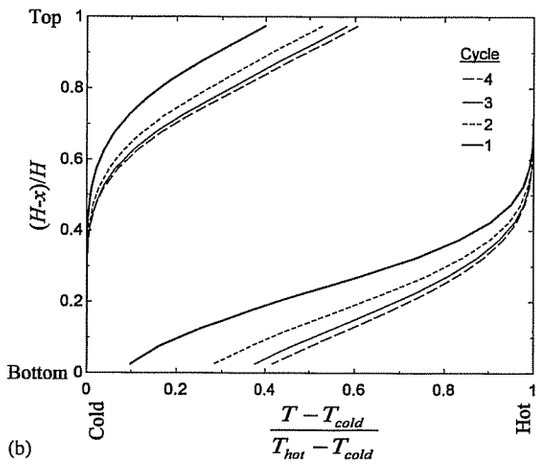

Figure 12. The development of temperature profiles within the thermocline tank over the course of four charge–discharge cycles for: (a) 600 nodes and (b) 20 nodes.

The tendency of the small node-count simulations of packed-bed thermocline storage systems to substantially reduce error over time demonstrates a mechanism through which errors incurred in predicting the performance of individual cycles can be self-corrective by augmenting the predicted performance of the cycles that follow. These long-term model dynamics demonstrate that the numerical precision required to predict the performance of a single storage system cycle is not a sufficient criterion to require the same level of numerical precision for a long-term simulation.

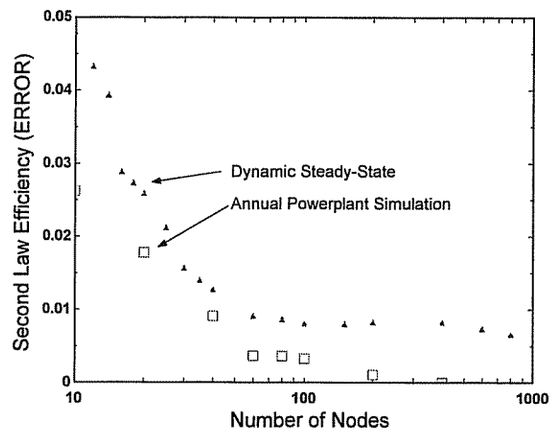

Figure 13. Error in the computation of second-law efficiency as a function of the number of numerical nodes for two cases: dynamic steady-state storage system second-law efficiency and second-law efficiency calculated during an annual power plant simulation.

The case considered thus far, a storage unit charged and discharged with constant periodic forcing functions, is a useful exercise but does not capture all of the variation and complexity inherent in any realistic system simulation. To reinforce the observations already made about the differences between single-cycle and long-term storage simulations, a year-long simulation of a solar thermal power plant with thermocline storage was run. This simulation uses the storage system model described in this section along with a parabolic trough solar field model and steam power cycle model developed by Patnode [18]. Based on weather data from Daggett, CA, the solar field produces heat transfer oil at constant temperature (400°C). The storage system is controlled to operate as a load-levelling device. That is, charging and discharging the storage system in order to maintain a constant flow rate of heat transfer oil to the power cycle. Figure 13 shows the results of this annual simulation compared to the dynamic steady-state data from Figure 11. For all levels of numerical precision considered, the annual simulation produced less error in second-law efficiency error than the dynamic steady-state values obtained with periodic forcing functions. This result implies that the highly varying storage system inputs that are part of a weather-driven

DOI: 10.1002/er

simulation have an additional self-corrective effect that, compounded over a year-long simulation, further reduces second-law efficiency error.

4. DISCUSSION

These simulations of water heating and thermal power systems represent two very different systems. In both cases, the behaviour of long-term simulations is insensitive to number of nodes although significant sensitivity is observed in short-term (e.g. 1 day) simulations. This effect may be explained by the following phenomena:

- The stratification of the tank implies the existence of three very distinct zones within the tank: a hot-temperature zone, a cold-temperature zone and the zone where the temperature gradient is present, as shown in Figure 14. Although the number of nodes affects the size of the zones within the tank, Figures 2 and 5 show that the size of the hot zones for tanks with different number of nodes is very similar. The similar size of the hot-temperature zones combined with the fact that the metrics used for assessing the performance of the system only consider as useful the hot region of the tank (i.e. it is detrimental to the behaviour of the system to use the fluid from the tank that is below a set temperature) result in a similar long-term performance of the tank with different number of nodes.
- The detailed governing equations for the one-dimensional representations of the tanks are derived from an energy balance on the tank. The fact that the results with a 1-node tank are very similar to the results with a tank with many nodes indicates that the basic principles are captured, even if the stratification is not well defined. For long-term simulations, the energy balance is the most important factor that governs the behaviour of the system. This behaviour is reinforced when typical weather data are used; variations in the boundary conditions apparently allow greater use of the energy that was left in the tank due to imperfect stratification during a previous cycle.

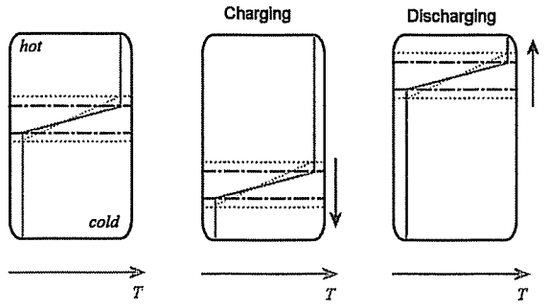

Figure 14. Three zones in a well-stratified tank. The dotted lines represent the variation in the predictions of the thermocline due to the number of nodes.

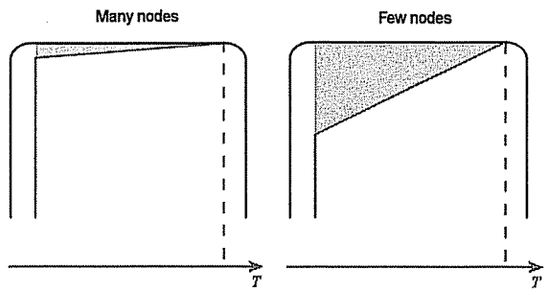

Figure 15. Temperature profile after discharge cycle. The shaded zone indicates the region of the tank whose temperature is above the low-temperature zone.

- Figure 12 shows that the temperature profiles obtained after several cycles are insensitive to the number of nodes that are used. This difference in temperature profiles may significantly affect the temperature near the top of the tank if the tank is almost fully discharged. This effect is shown in Figure 15, where the shaded zone indicates the zone of the tank that contains fluid above the low-temperature zone and that was not delivered during the present cycle. During the next charging cycle, the tank already has some energy stored and will be able to store additional energy. The net effect is that although during some cycles the coarse-grid tank does not discharge as much energy as the detailed-grid tank model, most of this energy is available for the next cycle. The final result is an effect through which errors incurred in predicting the performance of individual cycles can be

DOI: 10.1002/er

self-corrected by augmenting the predicted performance of the cycles that follow.

The major conclusion of this study is that only a relatively smaller number (e.g. five for a water storage tank) are needed to accurately simulate the annual performance of a solar system although this result is not evident from short-term simulations or experiments.

REFERENCES

1. Gari HN, Loehrke RI. A controlled buoyant jet for enhancing stratification in a liquid storage tank. *ASME Journal of Fluids Engineering* 1982; **104**(4):475–481.
2. Van Koppen CWJ, Thomas JPS, Veltkamp WB. Actual benefits of thermally stratified storage in a small and a medium size solar system. *Electric Power Research Institute (Report) EPRI EA*, 1979; 576–580.
3. Zurigat YH, Maloney KJ, Ghajar AJ. A comparison study of one-dimensional models for stratified thermal storage tanks. *Transactions of the ASME Journal of Solar Engineering* 1989; **111**:204–211.
4. Mavros P, Belessiotis V, Haralambopoulos D. Stratified energy storage vessels: characterization of performance, and modeling of mixing behavior. *Solar Energy* 1994; **52**(4):327–336.
5. Drück H, Heidemann W, Müller-Steinhagen H. Advanced storage concepts for solar combisystems. *EuroSun2004*, 20–23 June 2004.
6. Streicher W, Bales C. Combistores. In *Thermal Energy Storage for Solar and Low Energy Buildings*, Hadorn JC (ed.). International Energy Agency—Solar Heating and Cooling Task, vol. 32. International Energy Agency: Paris, 2005.
7. Kleinbach EM, Beckman WA, Klein SA. Performance study of one-dimensional models for stratified thermal storage tanks. *Solar Energy* 1993; **50**(2):155–166.
8. Duffie JA, Beckman WA. *Solar Engineering of Thermal Processes* (3rd edn). Wiley: New York, 2006.
9. Oberndorfer G, Beckman WA, Klein SA. Sensitivity of annual solar fraction of solar space and water heating systems to tank and collector heat exchanger parameters. *Proceedings of the 1999 ASES Conference*, Portland, ME, 1999.
10. Newton BJ. Modeling of solar storage tanks. *M.S. Thesis*, University of Wisconsin-Madison, 1995.
11. Klein SA *et al. TRNSYS, A Transient System Simulation Program, User's Manual, Version 16*, Solar Energy Laboratory, University of Wisconsin-Madison: Madison, WI, 2006.
12. Tanehhil JC, Anderson DA, Pletcher RH. *Computational Fluid Mechanics and Heat Transfer* (2nd edn). Taylor & Francis: London, 1997.
13. Celik I, Zhang WM. Calculation of numerical uncertainty using Richardson extrapolation: application to some simple turbulent flow calculations. *Journal of Fluids Engineering* 1995; **117**(3):439–445.
14. Schumann TEW. Heat transfer: a liquid flowing through a porous prism. *Journal of the Franklin Institute* 1929; **208**:405–416.
15. McMahan AC. Design & optimization of organic Rankine cycle solar-thermal powerplants. *M.S. Thesis*, University of Wisconsin-Madison, 2006.
16. Pacheco JE *et al.* Development of a molten-salt thermocline thermal storage system for parabolic trough plants. *Solar Energy Engineering* 2002; **124**:153–159.
17. Nellis GF, Klein SA. Regenerative heat exchangers with significant entrained fluid heat capacity. *International Journal of Heat and Mass Transfer* 2006; **49**: 329–340.
18. Patnode AM. Simulation and performance evaluation of parabolic trough solar power plants. *M.S. Thesis*, University of Wisconsin-Madison, 2006.

DOI: 10.1002/er